DEVELOPMENT OF A MUON LINAC FOR THE G-2/EDM EXPERIMENT AT J-PARC

M. Otani, N. Kawamura, T. Mibe, F. Naito, M. Yoshida, KEK, Oho, Tsukuba, 305-0801, Japan
K. Hasegawa, T. Ito, Y. Kondo, JAEA, Tokai, Naka, Ibaraki, 319-1195, Japan
N. Hayashizaki, Tokyo Institute of Technology, Tokyo, 152-8550, Japan
Y. Iwashita, Kyoto University, Kyoto, 611-0011, Japan
Y. Iwata, NIRS, Chiba, 263-8555, Japan
R. Kitamura, University of Tokyo, Hongo, 113-8654, Japan
N. Saito, J-PARC Center, Tokai, Naka, Ibaraki, 319-1195, Japan

Abstract

We are developing a linac dedicated to the muon acceleration for muon g-2/EDM experiment at J-PARC. The muon linac consists of a radio-frequency-quadrupole (RFQ), an inter-digital H-mode (IH) drift tube linac (DTL), a disk-and-washer (DAW) -type coupled cell linac (CCL), and a disk-loaded structure. This paper describes the design of each structure and current progress towards muon acceleration with the RFQ, which is expected to be the first practical realization of muon acceleration in the world.

INTRODUCTION

Though the discovery of the Higgs boson at LHC completed the discovery of all particles predicted by the Standard Model (SM) of elementary particle physics, some observations such as the existence of dark matter indicate new physics beyond SM at some energy scale or interaction scale. One of the clues for such new physics is the anomaly of the muon anomalous magnetic moment of $(g-2)_\mu$: a difference of approximately three standard deviations exists between the SM prediction and the measured value (with a precision of 0.54 ppm) of $(g-2)_\mu$ [1]. However, measurement with higher precision is necessary to confirm this anomaly. Low-emittance muon beams will facilitate more precise measurements, as the dominant systematic uncertainties in the previous experimental results are due to the muon beam dynamics in the muon storage ring.

At present, we are developing a muon linac for the $(g-2)_\mu$ experiment at the Japan Proton Accelerator Research Complex (J-PARC) [2] in order to realize a low-emittance muon beam. In the experiment, ultra slow muons with an extremely small transverse momentum of 3 keV/c (kinetic energy W = 25 meV) are generated via thermal muonium production [3] followed by laser dissociation [4]. The generated ultra slow muons are electro-statically accelerated to $\beta = v/c = 0.01$ (5.6 keV) and injected into the muon linac.

Figure 1 shows the muon linac configuration. In order to obtain a longitudinally bunched beam, a RFQ accelerator is employed for the first-stage acceleration. The operational frequency is chosen to be 324 MHz, in order to optimize the experiences at the J-PARC H^- RFQ. Although conventional linacs adopt Alvarez DTLs after RFQs, an IH-DTL is employed during the stage of particle velocity $\beta = 0.08$ to 0.28 (4.5 MeV) to yield a higher acceleration efficiency. After the muon is accelerated to $\beta = 0.28$, a DAW-type CCL is employed for effective acceleration. The operational frequency is chosen as 1.3 GHz because a 30 MW klystron, which was originally developed as the RF source for the KEKB linac [5], is applied for our project. Because the β variation is modest in the high-β region, the design emphasis has been shifted for achieving a high accelerating gradient, in order to realize a sufficiently short distance. Therefore, a disk-loaded structure is used for β greater than 0.7 (42 MeV).

The muon beam current is very small ($\sim 10^6$ muon paer second with 25 pulses per second). The pulse width is approximately 10 nsec, and the duty is also small.

In this paper, we describe the designs of each accelerator structure and the current progress towards muon acceleration.

LINAC DESIGN

RFQ

An RFQ is employed for initial acceleration ($\beta = 0.01 \sim 0.08$). In order to demonstrate the muon acceleration in a timely manner at a low cost, the existing RFQ that was originally developed as a J-PARC linac spare [6] is utilized. The RFQ was designed to accelerate H^-. In order to accelerate muons with the RFQ, the power is reduced to 1/80 of the design power. Figure 2 shows the beam evolution calculated by PERMTEQM [7] with the deduced power setting. The evolution shows good transmission (95%) for muons. The current progress towards actual muon acceleration with this RFQ is described in the next section. In addition, an RFQ dedicated to the acceleration of muons is being developed, the details of which can be found elsewhere [8]

IH-DTL

Inter-digital H-mode DTL [9, 10] is used for $\beta = 0.08$–0.28. In order to achieve high-efficiency acceleration, the alternative phase focusing (APF) scheme is employed [11–13]; in this scheme, transverse and longitudinal focusing are achieved with only the RF field, and no additional focusing element is necessary.

The APF IH-DTL for muons was designed [14] by LINAC-Sapf [15], CST MW Studio [16], and GPT [17]. First, the synchronous phase array is optimized for an idealized APF.

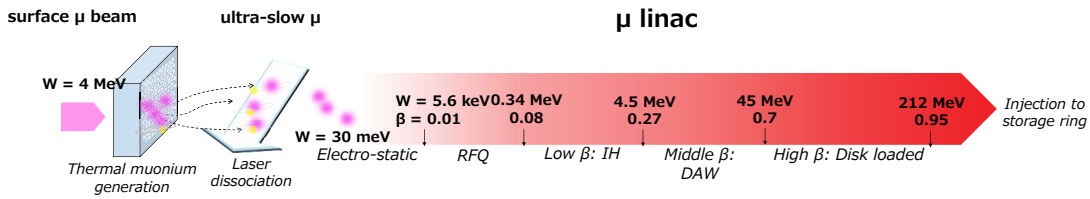

Figure 1: Configuration of low-emittance muon beam.

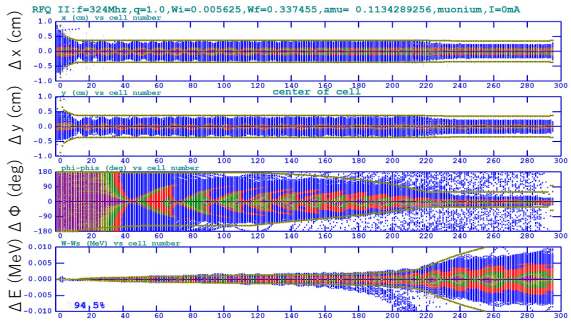

Figure 2: Evolution of the phase space distributions through the RFQ.

Then, the cells are arranged in the IH cavity in accordance with the optimized phase array. The RF acceleration field is optimized by tuning the IH cavity structures such as end ridge cut and cavity radius taper. Finally, the beam dynamics in the optimized field is numerically calculated.

Figure 3 shows the emittance growth along the beam axis calculated using GPT. The difference between the horizontal and vertical directions is due to the dipole field, which results in additional emittance growth in the vertical direction. The growth is still less than 20%, which is sufficiently small.

Currently detailed structures such as slug tuners are being designed for production [18].

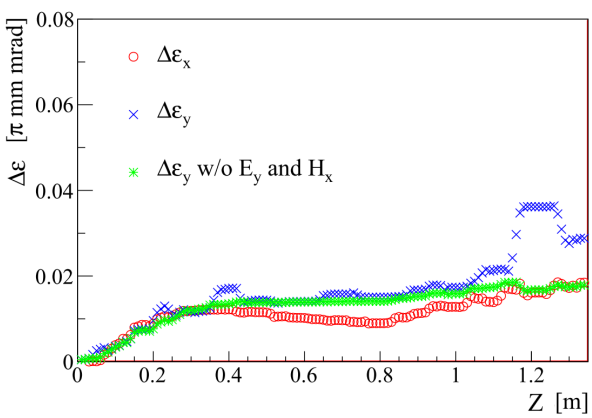

Figure 3: Emittance growth along beam axis.

DAW CCL

In the middle beta section ($\beta = 0.3 \sim 0.7$), the DAW cavity will be employed [19,20]. It has a high effective shunt impedance and high degree of coupling between adjacent RF cells. It is necessary to design a DAW cavity dedicated to the muon linac because muon acceleration has not been achieved thus far and a DAW cavity covering such a wide range of velocity is being developed for the first time.

The DAW cell was designed with SURPERFISH for the two-dimensional model and CST MW Studio for the three-dimensional model. In both models, the cavity structures are optimized to obtain a confluent condition ($f_a = f_b$), high shunt impedance (ZTT), and high average-to-peak field ratio. Because the DAW cell should be designed for several values of $\beta\lambda/4$, a semi-automatic algorithm for the cavity design optimization is constructed [21]. Then, all the optimization steps are repeated for several cavity lengths.

Figure 4 shows the dispersion curve for the model of $\beta = 0.3$. Because of bi-periodic structure, some stop bands appear at $\pi/2$. Though the TM11 mode is near the operational frequency, the cavity is tuned in the optimization process so that the operational frequencies lie in the stop band at $\pi/2$. Though the dipole mode passband TE11 crossed the line where the phase velocity matches the speed of muons, it is not considered a problem, because the muon beam current is negligibly small and transverse kick due to this mode is estimated to be much smaller than our requirement. Based on the optimized DAW cell model, a cold model fabricated in aluminum was designed. The model is being assembled and will be tested soon.

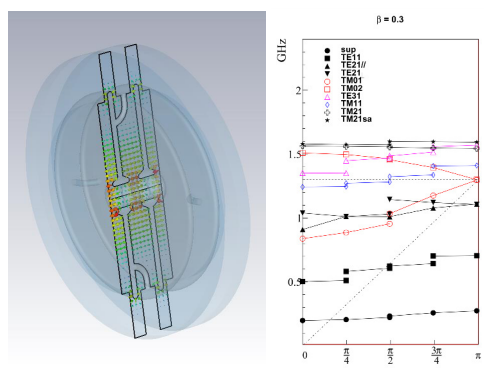

Figure 4: Dispersion curve with optimized cavity in several β calculated by CST MICROWAVE STDUIO.

The dynamics design was performed using PERMILA [22] and TRACE3D [23]. A tank consists of several DAW cells, and each tank is connected via a bridge coupler, where there is a doublet quadrupole magnet. The average acceleration field is set to 5.6 MV/m, which corresponds to 0.9 times the Killpatrick limit [24, 25] at the maximum field point. The number of DAW cells in a tank and the quadrupole strength are determined according to the beam instability; the zero-current phase advance in the first tank is less than 90°. Figure 5 shows the beam emittance along the DAW cells evaluated using PARMILA. The emittance growth is a few percent, which satisfies the requirement.

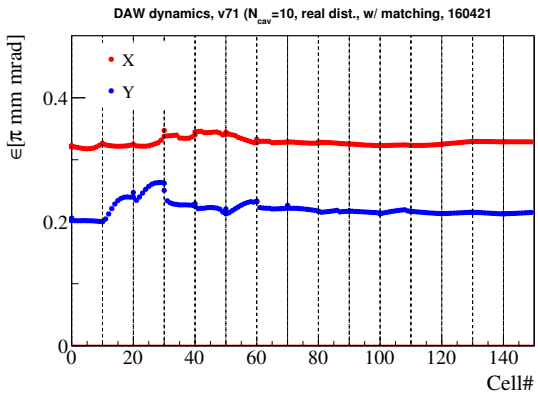

Figure 5: Emittance evolution in the DAW cavities.

Disk-loaded Structure

In order to achieve high-gradient acceleration, the acceleration structure is switched to a disk-loaded structure (DLS) from $\beta = 0.7$. Because the muon velocity still does not reach $\beta \sim 1$, the cell length should be gradually increased along the beam path. The cell was designed using SUPERFISH. Because the DLS is used in TW, the electro-magnetic fields are estimated by the superposition of the field calculated with two boundary conditions [26]. The beam dynamics is calculated using GPT. The acceleration gradient (E_0) is chosen as 20 MV/m. There are four acceleration modules and there is a focusing quadrupole pair in the modules. Figure 6 shows the phase space distributions of the output beam. The output emittances are 0.32 and 0.25 π mm mrad and further optimization will be performed by tuning the beam matching.

Design Summary

Table 1 shows the transverse emittance at the exit of each acceleration structure. As an initial acceleration simulation, the surface muon beam is simulated by g4beamline [27] according to the beamline design [28]. The simulation for the muonium production and diffusion is constructed in accordance with our experimental results [3]. The beam simulation from the ultra-slow muon production to the entrance of the RFQ is conducted using GEANT4 [29]. These realistic phase-space distributions are used for following accelerator simulations.

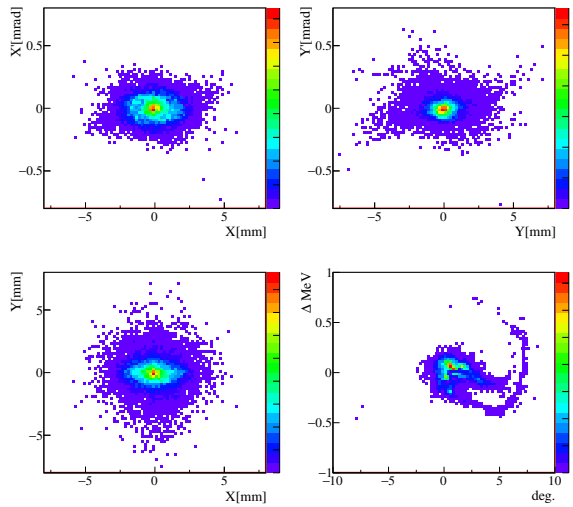

Figure 6: Phase distributions at the linac exit.

The output beam emittances are estimated to be 0.32 and 0.25 π mm mrad for the horizontal and vertical direction, respectively. The momentum spread of the output beam is calculated to be less than 0.1%. These values are comparable to the experimental requirement, and the efficiency of the injection to the muon storage ring is expected to be greater than 80% [30].

Table 1: Summary of the particle simulations though the muon linac.

	Initial	RFQ	IH-DTL	DAW	DL
Frequency [MHz]	-	324		1296	
Energy [MeV]	-	0.34	4.5	40	212
β	0.01	0.08	0.28	0.69	0.94
ε_x [π mm mrad]	0.38	0.30	0.32	0.32	0.32
ε_y [π mm mrad]	0.11	0.17	0.20	0.21	0.25
Transmission [%]	87	95	100	100	100
Decay loss [%]	17	19	2	4	1

CURRENT STATUS

In this section, the current progress towards the muon acceleration with RFQ (Fig. 7), which is expected to be the first case in the world, is presented.

Deceleration and Initial Acceleration

The muon deceleration and initial acceleration were performed at the J-PARC MLF test muon beamline (D-line) in February 2016. Figure 8 shows the experimental setup. The conventional surface muon beam is injected to a thin metal foil. Then, the decelerated muons [31] are accelerated by the SOA-type electro-static lens and transported by the electro-static components. Finally, the muons are detected by the detector system that consists of the microchannel plate (MCP) [32] and scintillator plates for decay positron

ISBN 978-3-95450-169-4

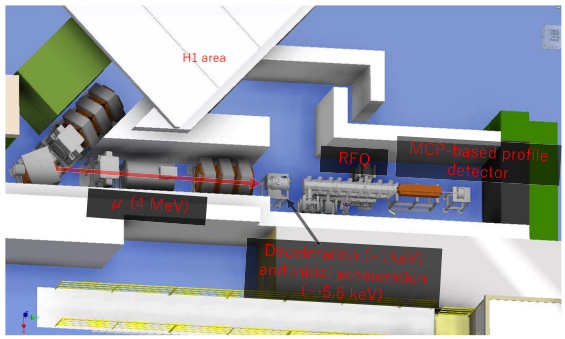

Figure 7: Setup for the muon acceleration with the RFQ.

detection. The details of the equipments and detectors can be found in [33].

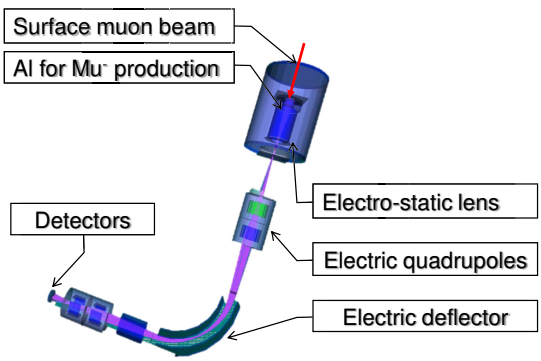

Figure 8: Setup of the SOA lens commissioning.

Figure 9 shows the event-timing distribution observed by the MCP detector. The dominant peak observed at ~ 2.8 μs is considered to be due to protons that were attached on the surface of the thin metal foil as hydrogens and knocked out from the surface by the muon beam injection. The predominant peak observed at ~ 0.8 μs is due to muon events, as the time of flight and the MCP pulse height distribution are matched to those of muons.

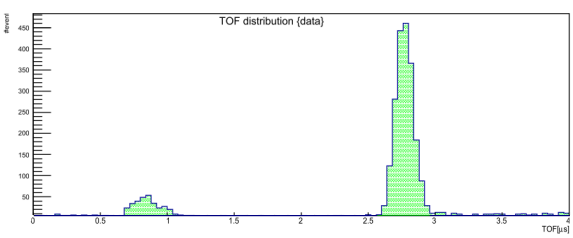

Figure 9: Event timing distribution observed by the MCP detector.

In conclusion, we succeeded in decelerating the muons with the thin meal foil and accelerating them with the SOA lens.

RFQ Commissioning

In order to verify the RFQ operation and measure the RF-related background, the RFQ offline test was performed in June 2015 in the J-PARC LINAC building.

Figure 10 shows photograph of the RFQ offline test setup. The MCP detector chamber is connected to the RFQ downstream. Vacuuming is performed with an ion pump, and the pressure reaches 10^{-6} Pa. The RFQ is powered on by a low-RF source and solid-state amplifier up to 6 kW and 25 Hz repetition. The forward, reflection waves and RFQ internal power are monitored by power meters.

Figure 10: Photo of the RFQ offline test at the J-PARC LINAC building.

Figure 11 shows the forward, reflection, and pick-up power in RFQ with nominal-power (5 kW) operation. The rising time is well consistent with the expectation based on the Q factor. Figure 12 shows the result of the MCP background measurement. Because the slow-muon-beam intensity in the first stage of the acceleration test is expected to be several counts per second, it is necessary to measure the background level with an accuracy comparable to that value. Though it was expected that there might be background events due to electrons or X-rays excited by the RF field, all the measurements are consistent with each other within a statistical error of about 0.1 Hz, and no background events are observed.

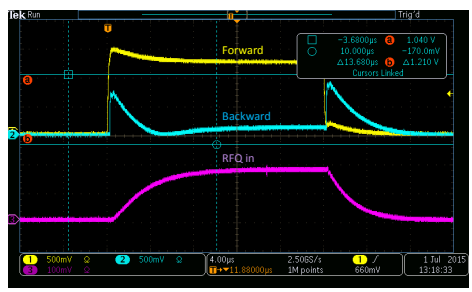

Figure 11: Forward, reflection wave and pick-up power in RFQ with a nominal power of 5 kW.

In conclusion, RFQ is successfully operated and accelerated muons can be measured using MCP without beam related background.

SUMMARY

Muon acceleration is required for precision measurement of $(g-2)_\mu$ with the low-emittance muon beam. The cell

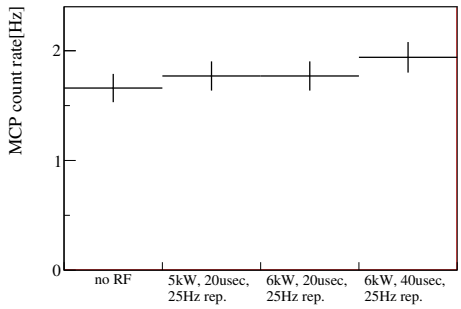

Figure 12: Result of the MCP background measurement. All the measurements are consistent with each other within statistical error.

design and dynamics design for all the acceleration structures were completed. The output beam emittance is estimated to be comparable to the experimental requirement. We are ready to perform muon acceleration with RFQ, which is expected to be the first case in the world. As soon as the new muon beamline at J-PARC MLF (H-line) [28] is constructed, the muon acceleration will be demonstrated.

ACKNOWLEDGMENT

It is a pleasure to thank the J-PARC LINAC group for assistance in the RFQ offline test. This work was supported by JSPS KAKENHI Grant Number 15H03666, 16H03987.

REFERENCES

[1] G.W. Bennett *et al.*, *Phys. Rev.* D73, 072003, 2006.

[2] J-PARC E34 conceptual design report, 2011. (unpublished)

[3] G.A. Beer *et al.*, *Prog. Theor. Exp. Phys.* 091, C01, 2014.

[4] P. Bakule *et al.*, *Nucl. Instru. Meth.* B266, 335, 2008.

[5] M. Kubosaki et al., *PASJ2011 Proc. (*Tsukuba, Japan, 2011), TUPS158.

[6] Y. Kondo et al., *Phys. Rev. ST Accel. Beams* 16, 040102, 2013.

[7] K. R. Crandall, T. P. Wangler, L. M. Young, J. H. Billen, G. H. Neuschaefer, and D. L. Schrage, Los Alamos National Laboratory Technical Report No. LA-UR-96-1836, 1996.

[8] Y. Kondo *et al.*, *Proc. of IPAC2015.* (Richmond, VA, USA, 2015), THPF045.

[9] P.M. Zeidlitz and V.A. Yamnitskii, *J. Nucl. Energy*, Part C4, 121, 1962.

[10] J. Pottier, *IEEE Trans. Nucl. Sci*. 16/3, 377, 1969.

[11] M.L.Good, *Phys. Rev.* 92, 538, 1953.

[12] S. Minaev and U. Ratzinger, *Proc. 1999 PAC Conf.*, (New York, US, 1999).

[13] Y. Iwata *et al.*, *Nucl. Instr. Meth*. A569, 685, 2006.

[14] M. Otani *et al.*, *Phys. Rev. Accel. Beam*s, 19, 040101, 2016.

[15] R.A. Jameson, arXiv:1404.5176[physics.acc-ph]

[16] CST Studio Suite, Computer Simulation Technology (CST). [https://www.cst.com/products/CSTMWS]

[17] General Particle Tracer, Pulsar Physics. [http://www.pulsar.nl/gpt/]

[18] M. Otani *et al.*, *PASJ2016 Proc*. (Chiba, Japan, 2016), TUP017.

[19] H. Ao *et al.*, *Jpn. J. Appl. Phys*. Vol. 39 (2000) 651-656

[20] M. Otani *et al.*, *PASJ2015 Proc*. (Tsuruga, Japan, 2015), WEOM02.

[21] M. Otani *et al.*, *Proc. of IPAC2016*. (Busan, Korea, 2016), TUPMY04.

[22] Los Alamos Accelerator Code Group (LAACG), LANL, Los Alamos, [http://www.laacg.lanl.gov].

[23] K.R. Crandall and D.P. Rustoi, Los Alamos Report, No. LA-UR-97-886, 1997.

[24] W.D. Kilpatrick, *Rev. Sci. Instr.* 28, 824, 1957.

[25] T.J. Boyd Jr., Kilpatrick's Criterion, Los Alamos Group AT-1 report AT-1:82-28, 1982.

[26] M.Yamamoto, [http://www.yamamo10.jp/yamamoto/study/accelerator/GPT/TW_structure/index.php.]

[27] G4beamline, Muons, Inc. [http://www.muonsinternal.com/muons3/G4beamline]

[28] M. Otani for the E34 collaboration, *Proc. of the 2nd International Symposium on Science at J-PARC* (Tsukuba, Ibaraki, Japan), 025010, 10.7566/JPSCP.8.025010.

[29] J. Allison *et al.*, *IEEE Transactions on Nuclear Science* 53 No. 1 (2006) 270-278.

[30] H. Iinuma, H. Nakayama, K. Oidea, K. Sasaki, N. Saito, T. Mibe, and M. Abe, *Nucl. Instr. and Meth. in Phys. Re*s. A 832 51-62 (2016).

[31] Y. Kuang et al., *Phys. Rev.* A39, 6109, 1989.

[32] Hamamatsu microchannel plate. [https://www.hamamatsu.com/jp/en/3008.html]

[33] M. Otani et al., *Proc. of IPAC2015.* (Richmond, VA, USA, 2015), WEPWA023.

ISBN 978-3-95450-169-4